Bordetella pertussis FbpA Binds Both Unchelated Iron and Iron Siderophore Complexes

Sambuddha Banerjee,[†] Aruna J. Weerasinghe,[†] Claire J. Parker Siburt,[†] R. Timothy Kreulen,[†] Sandra K. Armstrong,[‡] Timothy J. Brickman,[‡] Lisa A. Lambert,[§] and Alvin L. Crumbliss*,[†]

[†]Department of Chemistry, Duke University, Durham, North Carolina 27708, United States
[‡]Department of Microbiology, University of Minnesota, Minneapolis, Minnesota 55455, United States
[§]Department of Biology, Chatham University, Pittsburgh, Pennsylvania 15232, United States

S Supporting Information

ABSTRACT: *Bordetella pertussis* is the causative agent of whooping cough. This pathogenic bacterium can obtain the essential nutrient iron using its native alcaligin siderophore and by utilizing xeno-siderophores such as desferrioxamine B, ferrichrome, and enterobactin. Previous genome-wide expression profiling identified an iron repressible *B. pertussis* gene encoding a periplasmic protein (FbpA$_{Bp}$). A previously reported crystal structure shows significant similarity between FbpA$_{Bp}$ and previously characterized bacterial iron binding proteins, and established its iron-binding ability. *Bordetella* growth studies determined that FbpA$_{Bp}$ was required for utilization of not only unchelated iron, but also utilization of iron bound to both native and xeno-siderophores. In this *in vitro* solution study, we quantified the binding of unchelated ferric iron to FbpA$_{Bp}$ in the presence of various anions and importantly, we demonstrated that FbpA$_{Bp}$ binds all the ferric siderophores tested (native and xeno) with μM affinity. *In silico* modeling augmented solution data. FbpA$_{Bp}$ was incapable of iron removal from ferric xeno-siderophores *in vitro*. However, when FbpA$_{Bp}$ was reacted with native ferric-alcaligin, it elicited a pronounced change in the iron coordination environment, which may signify an early step in FbpA$_{Bp}$-mediated iron removal from the native siderophore. To our knowledge, this is the first time the periplasmic component of an iron uptake system has been shown to bind iron directly as Fe^{3+} and indirectly as a ferric siderophore complex.
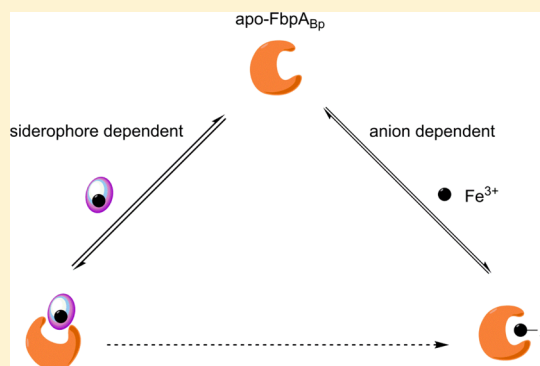
I ron is the second most abundant metal in the Earth's crust and is critical for many life processes despite its extreme insolubility and toxicity under physiological conditions.[1] Thus, biological systems have developed specialized mechanisms for transport, storage, and uptake of this essential nutrient. To obtain iron, many bacteria produce siderophores that bind extracellular iron, diffuse to the bacterial surface, and are taken up via specific receptor proteins.[2−6] Certain bacteria can also utilize siderophores produced by other microbial species (xeno-siderophores) if they produce the cognate transporters. Heme can also serve as an iron source,[7,8] and some bacteria can utilize host transferrin- or lactoferrin-bound iron.[9−12] In Gram-negative bacteria, iron sources are typically bound by an outer membrane receptor (OMR) and transported to the periplasm using energy supplied by the TonB complex.[13] A substrate-specific periplasmic binding protein (PBP) interacts with the iron source, binds the cargo between two lobes, and delivers it across the periplasm to the appropriate ATP-binding cassette (ABC) transporter for transit to the cytoplasm.[14−16]

The PBPs involved in bacterial iron uptake have historically been classified as either unchelated iron binders or chelated iron binders (i.e., iron-siderophore complex binders).[14,17−19] However, the unchelated iron binders are not always categorized together. (Unchelated iron has variously been referred to in the literature as naked or inorganic iron in reference to direct binding to the +3 ion.) One prototypical unchelated iron binder is the periplasmic ferric iron binding protein FbpA$_{Ng}$ from *Neisseria gonorrheae*.[20] FbpA$_{Ng}$ is required for utilization of host-transferrin-derived iron and binds Fe^{3+} directly in the first coordination shell in the presence of a requisite synergistic anion.[10,19−24] Unchelated iron binding proteins from other bacteria, including some that do not produce transferrin or lactoferrin receptors, have also been shown to bind iron directly. However, the anion-dependence, iron-coordination geometry, and type of amino acid side chains involved in iron sequestration vary.[14,25−28] It has been shown that even among homologues of FbpA$_{Ng}$, direct iron binding is accomplished in a variety of ways by bacteria that use a variety of iron sources.[26] On the other hand, one prototypical binder of chelated iron is the iron-siderophore binding PBP FhuD from *Escherichia coli*.[29−31] The reported crystal structures of FhuD

show that the first coordination shell of iron is occupied by the siderophore, and the protein occupies the second coordination shell.[29]

The schemes currently used to categorize protein families, of which the periplasmic components of iron uptake systems are members, use a variety of classification criteria, but all imply separate functions: either unchelated iron transport or iron-siderophore transport.[7,18] *Here we report a novel capacity for a periplasmic protein that is involved in iron uptake in Bordetella pertussis: the ability to bind iron directly and the ability to bind iron-siderophore complexes.*

The Gram-negative bacterial species *B. pertussis* is a respiratory pathogen that causes whooping cough in humans.[32,33] *B. pertussis* can acquire iron using its heme uptake system[34] or its native dihydroxamate siderophore alcaligin (ALC; Figure S1 in Supporting Information [SI]).[35,36] It can also use xeno-siderophores, including desferrioxamine B (DFB), ferrichrome (FC),[37] and enterobactin (ENT), among others (Figure 1; Figure S1 in SI).[38] Of the *Bordetella*
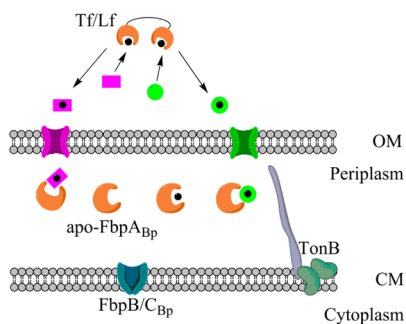
Figure 1. *Bordetella* FbpA-dependent iron uptake via alcaligin (pink rectangles) and xeno- (e.g., ENT, DFB, FC; green circle) siderophores. Host iron sources include transferrin or lactoferrin (Tf/Lf) as well as others not shown. TonB-dependent receptors (green and pink) are shown in the outer membrane (OM); the TonB complex and the ABC transporter $FbpB/C_{Bp}$ are in the cytoplasmic membrane (CM). $FbpA_{Bp}$ is shown in the periplasm, and a previous study showed that it is important in unchelated iron and iron-siderophore utilization.[42]

siderophore systems, only the ALC and ENT systems have been characterized.[39,40] The ALC genes encode ALC biosynthesis, export and regulation activities, and the OMR.[39] The ENT gene cluster encodes the OMR, an IroE hydrolase orthologue, and a transcriptional regulator.[40] Notably, there are no genes predicted to encode cognate periplasmic iron-siderophore binders (or ABC transporters) within the ALC and ENT chromosomal gene clusters.

Recently, we identified *fbpA* as an iron repressible *B. pertussis* gene that is also present in other *Bordetellae*.[42] *fbpA* encodes a periplasmic protein ($FbpA_{Bp}$) with significant structural similarity to iron binding proteins from *Serratia marcescens*, *Neisseria* spp., and *Haemophilus influenzae*.[13,16,17] *B. pertussis fbpA* is predicted to be cotranscribed with *fbpB* and *fbpC*, which encode the permease and ATPase components of an ABC transporter. *B. pertussis fbpA* mutants were defective in using unchelated iron for growth and, remarkably, were also defective in using the native siderophore and xeno-siderophores for growth.[42] Heme iron assimilation was not affected by *fbpA* inactivation. Since the prototypic bacterial siderophore system relies on a siderophore-specific PBP and associated ABC transporter, these *Bordetella* results were unusual as ALC, ENT, DFB, and FC are quite structurally different (Figure S1 in SI).

Not only are their functional groups different, but the hexadentate siderophores ENT, DFB, and FC bind iron in a 1:1 ratio, whereas tetradentate ALC binds iron in a 2:3 ratio (Fe^{3+}:ALC) at physiological pH (see SI).[4,36,43,44] These results suggested that $FbpA_{Bp}$ interacts with diverse ferric siderophores to mediate iron transport to the cytosol. To our knowledge, a PBP capable of binding iron directly and capable of binding iron-siderophore complexes has not been described previously. The biological purpose of direct interaction with iron by a PBP involved in iron-siderophore utilization may represent a new paradigm for PBP function.

The X-ray crystal structures of apo-$FbpA_{Bp}$ (PDB: 1Y9U), Fe−$FbpA_{Bp}$−carbonate (PDB: 2OWT), and Fe−$FbpA_{Bp}$−(oxalate)$_2$ (PDB: 2OWS) have been reported and show that $FbpA_{Bp}$ can directly coordinate Fe^{3+} through its conserved tyrosine residues (Y143, Y199, and Y200).[26,27] Similar to $FbpA_{Ng}$,[20] the crystal structures of $FbpA_{Bp}$ show iron bound directly by the protein with an anion present.[26,27] These solid state studies of $FbpA_{Bp}$, coupled with its known requirement for ferric siderophore utilization,[26,27,42] indicate that $FbpA_{Bp}$ is similar to other unchelated iron binders, but also has potentially unique functions in ferric siderophore utilization.

In this study, using $FbpA_{Bp}$ produced naturally in *Bordetella* cells, we quantified Fe^{3+} sequestration by $FbpA_{Bp}$ in the presence of various synergistic anions in solution. We also demonstrated that $FbpA_{Bp}$ binds ferric complexes of ALC, ENT, DFB, and FC, all with micromolar affinity, and characterized those binding interactions in solution. This report describes *B. pertussis* $FbpA_{Bp}$ as the first known example of a promiscuous periplasmic iron transport component that binds both unchelated iron and ferric siderophores and thus may act as a nodal point in non-heme *Bordetella* iron transport.

■ EXPERIMENTAL METHODS

Materials. All chemicals used were of highest purity grade: MES (2-(N-morpholino)ethanesulfonic acid) buffer, desferrioxamine B mesylate salt, and ferrichrome solution (iron free, from *Ustilago sphaerogena*) (Sigma Chemicals); sodium chloride, sodium carbonate (Fisher Chemical); sodium oxalate (Allied Chemical); sodium citrate (J. T. Baker); and sodium NTA (Aldrich Chemical Co.). Iron-free 50 mM MES, 100 mM NaCl buffer solutions were prepared in acid-washed buffer bottles by dissolving the required amount of MES and NaCl in deionized water, and the pH was adjusted to 6.5 by addition of acid/alkali. Chelex 100 (BioRad) beads were added to this solution to remove iron contamination and left overnight followed by filtration to remove the beads. All experiments were performed in pH 6.5 buffer as the pH of the periplasm is believed to be slightly acidic relative to the surroundings.[45,46] Apo-alcaligin and enterobactin were purified as described previously, from supernatant fluids of *Bordetella bronchiseptica* and *E. coli*, respectively.[36,41,47]
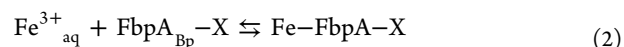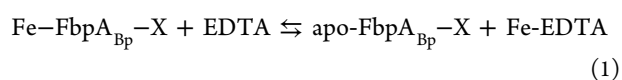
Purification of $FbpA_{Bp}$. *B. bronchiseptica* strain BRM72 ($\Delta fbpA$) carrying plasmid pBBR/$fbpA_{Bp}$ encoding *fbpA* from *B. pertussis* strain Tohama I was used to produce the $FbpA_{Bp}$ protein in the periplasm under natural iron starvation conditions. Bacteria were cultured in iron-depleted Stainer−Scholte medium,[48] containing 0.5% casamino acids and gentamicin (10 μg/mL) at 35 °C. $FbpA_{Bp}$ was extracted from the bacteria by osmotic shock treatment as described previously.[49] The osmotic shock fraction was clarified by centrifugation, followed by filtration using a low protein binding polyethersulfone membrane filter with 0.2 μm pore

size. The clarified osmotic shock fraction was dialyzed against 10 mM Tris buffer, pH 8.6, at 4 °C, and applied to a 2.5 cm × 15 cm DEAE CL-6B Sepharose anion-exchange column. The column was washed with 10 bed volumes of 10 mM Tris buffer, pH 8.6, then eluted with a 4-bed volume continuous gradient of 0.0−0.5 M NaCl. Peak fractions were pooled and dialyzed against 10 mM Tris buffer, pH 8.6. Purified FbpA$_{Bp}$ was concentrated by ultrafiltration and the protein concentration was determined using the Bradford method with bovine serum albumin as the standard.[50] The identity of the FbpA$_{Bp}$ protein was confirmed by liquid chromatography−tandem mass spectrometry (80% coverage, 100% protein identification probability) using an LTQ ion trap mass spectrometer. An SDS-PAGE gel showing FbpA$_{Bp}$ is presented in the SI as Figure S10.

Preparation and Characterization of Fe-FbpA$_{Bp}$−X Assemblies. UV−vis spectra were recorded using a Cary-50 UV−vis spectrophotometer with 1 cm path length cells in 50 mM MES, 100 mM NaCl at pH 6.5 and room temperature. The molar absorptivity of holo-FbpA$_{Bp}$ was calculated on the basis of the absorbance band at 280 nm from an iron-loaded FbpA$_{Bp}$ sample (ε = 44000 M^{-1} cm^{-1}) and the characteristic absorbance band in the visible region of the spectrum in the presence of various anions. The molar absorptivity of apo-FbpA$_{Bp}$ is 38500 M^{-1} cm^{-1} at 280 nm and is ∼10% lower than that of holo-FbpA$_{Bp}$ following a trend reported by us for FbpA$_{Ng}$ in a previous study.[23]

Fe−FbpA$_{Bp}$−X (X = carbonate or oxalate) was prepared by adding 50 equiv of Na-carbonate or oxalate from freshly prepared stock solutions (50 mM) to apo-FbpA$_{Bp}$ in 50 mM MES, 100 mM NaCl at pH 6.5. The resulting solutions were allowed to equilibrate for 30 min before 10 equiv of standardized Fe(ClO$_4$)$_3$ solution were added, and the solutions were gently mixed for 30 min and then allowed to stand overnight at 4 °C to precipitate any unreacted iron, which was removed by filtration with a syringe-driven 0.2 μM filter unit (Corning Corporation). Fe−FbpA$_{Bp}$−citrate was prepared by adding 10 equiv of Na-citrate from a freshly prepared stock solution (20 mM) to apo-FbpA$_{Bp}$ followed by 2 equiv of Fe-citrate (1:1, 2 mM). Similarly, to prepare Fe−FbpA$_{Bp}$−NTA, 10 equiv of Na-NTA from a stock solution (20 mM) were added to apo-FbpA$_{Bp}$ followed by the addition of 2 equiv of Fe-NTA (1:1, 2 mM). Additional Fe(ClO$_4$)$_3$/Fe-citrate/Fe-NTA was titrated into the solutions of protein complexes until no further increase in intensity of the corresponding charge transfer band was observed, ensuring fully iron-loaded protein complex formation. Formation of the corresponding ternary complexes was confirmed by the appearance of well-resolved charge transfer bands in the visible region of the absorption spectrum of the respective Fe−FbpA$_{Bp}$−X species (X = citrate, carbonate, oxalate, or NTA). All protein complexes were dialyzed against 50 mM MES, 100 mM NaCl at pH 6.5 buffer three times using Slide-A-Lyzer dialysis cassette (Thermo Scientific) to remove excess iron and anion.

A competitive equilibrium between Fe−FbpA$_{Bp}$−X (X = oxalate, carbonate, citrate, or NTA) and EDTA (eq 1) was employed to determine the Fe^{3+} binding constants of ternary complexes for Fe−FbpA$_{Bp}$−X, as defined in eq 2, using Experimental Methods described previously.[23]

$$\text{Fe−FbpA}_{Bp}\text{−X} + \text{EDTA} \leftrightarrows \text{apo-FbpA}_{Bp}\text{−X} + \text{Fe-EDTA} \tag{1}$$

$$\text{Fe}^{3+}{}_{aq} + \text{FbpA}_{Bp}\text{−X} \leftrightarrows \text{Fe−FbpA−X} \tag{2}$$

Characterization of apo-FbpA$_{Bp}$ Interactions with Ferric Siderophores. Fluorescence spectroscopy was used to quantitatively determine the interaction between apo-FbpA$_{Bp}$ and ferric siderophores. All fluorescence spectra were recorded on JOBIN-YVON-SPEX Fluorolog3 fluorimeter at right angle mode with 5 nm slit width and in 50 mM MES, 100 mM NaCl buffer at pH 6.5 and room temperature. To minimize the intrinsic emission from the tyrosine residues, the apo-FbpA$_{Bp}$ was excited at 297 nm. The observed intrinsic emission from apo-FbpA$_{Bp}$ is the summation of emissions from individual tryptophan residues and is centered at 352 nm under our experimental conditions. This indicates a hydrophilic environment on average for the four tryptophan residues present in FbpA$_{Bp}$.[51,52] Quenching of the intrinsic tryptophan emission band upon ligand (Fe^{3+}-siderophore) addition is an indication of reduction in the concentration of the free apo-FbpA$_{Bp}$ in solution that can emit at 352 nm, and these data were used to determine the binding affinity of FbpA$_{Bp}$ with various Fe^{3+}-siderophores. An apparent Fe^{3+}-siderophore/apo-FbpA$_{Bp}$ dissociation constant (K_d) corresponding to the equilibrium in eq 3 was determined by fluorescence titration using eq 4, where P represents FbpA$_{Bp}$, Fe-sid represents both ferric native and ferric xeno-siderophores and P(Fe-sid) represents the FbpA$_{Bp}$(Fe-siderophore) complex. Reproducible results were only obtained for a one-site binding model. The experimental design and data analysis approach was the same as

$$\text{FbpA}_{Bp}(\text{Fe-sid}) \leftrightarrows \text{apo-FbpA}_{Bp} + \text{Fe-sid} \tag{3}$$

$$K_d = [\text{P}]_{eq}[\text{Fe-sid}]_T/[\text{P(Fe-sid)}]_{eq} \tag{4}$$

that used previously by us and others.[22,31,52,53] K_d values were obtained from plots of eq 5, where Q% is the observed % quenching at each point in the titration and Q_{max} is the maximum % quenching.[22]

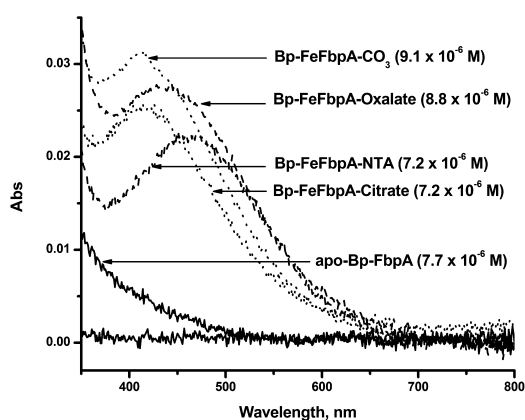$$Q\% = Q_{max}[\text{Fe-sid}]_T/\{K_d + [\text{Fe-sid}]_T\} \tag{5}$$

A possible exchange of Fe^{3+} between Fe-siderophores and apo-FbpA$_{Bp}$ was monitored using UV−visible spectroscopy by monitoring the CT band of the Fe-siderophore over a 6 h time period (protein:ferric xeno-siderophore 1:2; protein:ferric native siderophore = 2:1).

Protein Modeling. Iron and siderophore binding sites were modeled starting with RCSB Protein Data Bank structures 1Y9U:A and 2OWT (to which hydrogens were added).[26] 1Y9U is the structure for the *B. pertussis* ferric binding protein in the apo (open) conformation. 2OWT represents the holo (closed) structure, and its ligands, CO$_3$$^{2-}$ and iron, were removed before docking. Ligands for docking were downloaded from either RCSB Protein Data Bank (www.rcsb.org) or, in the case of ferrioxamine B[54] and ferric-alcaligin (Fe$_2$ALC$_3$),[43] and the alcaligin monomer (ALC), from the Cambridge Crystallographic Data Centre (reference codes: 155586, TEQKUV, and C00080, respectively). Patchdock[55] was used to find the initial docking sites, and models were fine-tuned with Chimera.[56] The superposition of the alcaligin (monomer)-bound model with the 2OWS structure was created with the Matchmaker utility implemented in Chimera. Models were evaluated using ERRATv2,[57] and the best scoring value for each is reported.

■ RESULTS AND DISCUSSION

Crystal structures of holo-FbpA$_{Bp}$ established that it binds Fe^{3+} directly in the presence of synergistic anions (oxalate and carbonate),[26,27] and *Bordetella* growth studies showed that FbpA$_{Bp}$ is essential for the utilization of Fe^{3+} bound to multiple structurally distinct siderophores.[42] The flexibility of the β-sheet hinge region of FbpA$_{Bp}$ is consistent with the possibility of such substrate binding promiscuity. Modeling of ferric native and xeno-siderophore binding between the two lobes of FbpA$_{Bp}$ (Figures S2−S5 in SI) predicted favorable binding interactions, supporting the possibility that FbpA$_{Bp}$ can act as a ferric siderophore chaperone. In the following sections we describe the interaction of FbpA$_{Bp}$ with unchelated Fe^{3+} and with iron-siderophore complexes utilized by *Bordetella*.

FbpA$_{Bp}$ Strongly Sequesters Unchelated Fe^{3+} in the Presence of Various Synergistic Anions. Crystal structures reported for Fe−FbpA$_{Bp}$−(oxalate)$_2$ and Fe−FbpA$_{Bp}$−carbonate show that Fe^{3+} is bound to the three conserved tyrosine residues on the C-lobe of the protein.[26,27] Until now there has been no report that quantifies FbpA$_{Bp}$−Fe^{3+} binding interactions. Here we have determined the Fe^{3+} affinity of each Fe−FbpA$_{Bp}$−X assembly, where X is citrate, carbonate, oxalate, or nitrilotriacetate (NTA). Figure 2 shows a

Figure 2. Visible region spectra of Fe-FbpA$_{Bp}$-X (X = citrate, carbonate, oxalate, or NTA) in 50 mM MES, 100 mM NaCl at pH 6.5. Protein concentrations are indicated.

representative overlay of the visible spectra for all Fe−FbpA$_{Bp}$−X assemblies prepared individually as described in Experimental Methods, indicating the anion promiscuity of FbpA$_{Bp}$ in sequestering Fe^{3+} and modulation of the position of the charge transfer (CT) bands by various anions (Table 1). No Fe^{3+} sequestration was observed in the absence of a suitable synergistic anion. *In silico* modeling also identified an arginine

Table 1. Biophysical Characterization of Fe-FbpA$_{Bp}$-X (X = Citrate, Carbonate, Oxalate, or NTA) at pH 6.5 in 50 mM MES, 100 mM NaCl

anion	λ_{max}, nm	ε, M^{-1} cm^{-1}	K'_{eff}, M^{-1a}
citrate	410	3433	$7.0 \pm 3.7 \times 10^{16}$
NTA	466	3049	$4.7 \pm 2.0 \times 10^{16}$
oxalate	440	3143	$5.5 \pm 1.2 \times 10^{16}$
carbonate	412	3390	$1.2 \pm 0.03 \times 10^{16}$

^{a}Effective stability constants corresponding to eq 2. Values reported represent the variation in two independent determinations.

residue (R105) involved in anion binding in other FbpA$_{Bp}$ homologues (Table S1 in SI) that is conserved in FbpA$_{Bp}$. The appearance of characteristic CT bands that are unique for different anions indicates that these anions directly participate in iron sequestration at the first coordination shell and are synergistic anions.

The observed Fe^{3+} affinity constants (K'_{eff}) defined in eq 2 and determined as described in Experimental Methods are listed in Table 1. K'_{eff} values ($\sim$10^{16} M^{-1}) are approximately 1−2 orders of magnitude less than those reported for FbpA$_{Ng}$, which may be due to a difference in coordination environment provided by these two proteins.[23,26,27,58]
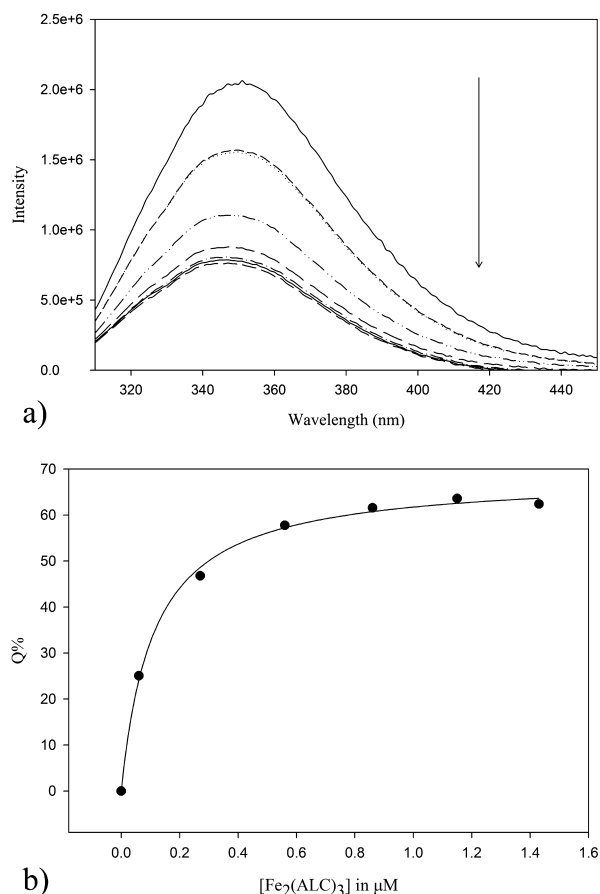
We conclude that FbpA$_{Bp}$ is capable of sequestering Fe$^{3+}_{aq}$ with high affinity ($K'_{eff} \approx 10^{16}$ M^{-1}) in the presence of various synergistic anions. In these assemblies, the anions and the protein both occupy the first coordination shell of Fe^{3+}.

FbpA$_{Bp}$ Binds Ferric Siderophore Complexes. Our hypothesis based on *Bordetella* growth experiments using *fbpA* mutants[42] and *in silico* modeling (Figures S2−S5 in SI) proposed that FbpA$_{Bp}$ has the potential to bind ferric native and xeno-siderophores as illustrated in eq 3. To investigate this possible interaction we carried out fluorescence quenching titrations involving apo-FbpA$_{Bp}$ and ferric-alcaligin, or one of the ferric xeno-siderophores. Apo-FbpA$_{Bp}$, with four tryptophan residues in its structure, emits at 352 nm when excited at 297 nm, indicating a hydrophilic average environment for the tryptophans.[51] Although both ferric native and xeno-siderophores showed concentration-dependent quenching of the intrinsic emission band, the concentration dependence, change in band position, and maximum quenching (Q_{max}) differed appreciably between the two types of siderophores. This suggests a differential mode of interaction between FbpA$_{Bp}$ and the ferric native siderophore versus the ferric xeno-siderophores. The affinities (K_d; eq 3) of all the holo-siderophores for FbpA$_{Bp}$ were calculated using these concentration dependent quenching data as described in Experimental Methods. Figure 3a shows representative quenching spectra when Fe$_2$(ALC)$_3$ was titrated into a solution of apo-FbpA$_{Bp}$, and Figure 3b shows the fit of these data using a one site binding model.

The K_d value for Fe$_2$(ALC)$_3$ binding to apo-FbpA$_{Bp}$ is 0.13 ± 0.04 μM. Similar micromolar affinity for ferric-hydroxamate siderophore binding to FhuD from *E. coli* has been reported.[31] Figure 3a shows an ~8 nm blue shift in the emission band, indicating a change in average tryptophan environment from hydrophilic to hydrophobic surroundings.[51] Consequently, we conclude that addition of Fe$_2$(ALC)$_3$ to apo-FbpA$_{Bp}$ leads to a change of conformation of FbpA$_{Bp}$ concomitant with a change in tryptophan hydrophilicity.

K_d values calculated using the same mathematical model for the ferric xeno-siderophores (ENT, DFB, and FC) were found to be an order of magnitude higher than the K_d calculated for Fe$_2$(ALC)$_3$ ($K_d \approx 1$ μM). Representative data are presented in SI (Figures S6−S8). The Q_{max} for the xeno-siderophore titrations range from 20 to 60%, whereas for the Fe$_2$(ALC)$_3$ titration Q_{max} is 80%. We interpret this as indicative of the involvement of the tryptophan residues (or a subset) to a greater extent for the protein−ligand interaction in the presence of Fe$_2$(ALC)$_3$ than for the ferric xeno-siderophores.

When the apo-siderophores (ALC and ENT, as representative hydroxamate and catecholate siderophores, respectively) were titrated into a solution containing apo-FbpA$_{Bp}$ in separate experiments (final protein:apo-siderophore = 1:4 and 1:2,

Figure 3. (a) Representative fluorescence emission spectra for FbpA$_{Bp}$ (1 μM) in the presence of increasing concentrations of Fe$_2$(ALC)$_3$ (0–2 μM). Upon addition of Fe$_2$(ALC)$_3$, emission decreases and a blue shift of ~8 nm is observed. Refer to the Experimental Methods section for experimental conditions. (b) A plot of Q% FbpA$_{Bp}$ fluorescence emission (352 nm) vs increasing [Fe$_2$(ALC)$_3$]. Filled circles represent actual data points, and the smooth line is the best fit of eq 5 to the data. Average K_d for eq 3 = 0.13 ± 0.04 μM and Q_{max} = ~80%.

respectively), the apo-protein fluorescence emission band did not show significant quenching (<16%; Figure S9 in SI). This suggests that only a very weak interaction occurs between these apo-siderophores and the apo-protein. A similar result was obtained when a UV–vis spectral difference experiment was performed between apo-DFB and apo-FbpA$_{Bp}$ (results not shown), once again indicating that the apo-protein is not able to bind an apo-siderophore effectively. These experiments suggest that the "binding interaction" that we observe quantitatively using a fluorescence emission quenching assay for holo-siderophores and apo-FbpA$_{Bp}$ is ligand-conformation specific and in fact requires the siderophore to be bound to Fe^{3+}.

These results indicate that in addition to binding directly to unchelated Fe^{3+}, FbpA$_{Bp}$ can bind the native ferric siderophore (ALC) with K_d = ~0.1 μM and various ferric xeno-siderophores with K_d = ~1.0 μM. This finding is consistent with earlier growth studies demonstrating that *Bordetella fbpA* mutants are impaired in their utilization of ferric siderophores as well as unchelated iron.[42] These results also support our hypothesis derived from *in silico* modeling (Figures S2–S5 in SI) and represent the first quantification of the capacity of a bacterial periplasmic protein to bind iron both directly and indirectly.

Fe^{3+} Exchange within the FbpA$_{Bp}$/holo-Siderophore Assembly. The fact that FbpA$_{Bp}$ can bind unchelated Fe^{3+} with high affinity (Table 1) and can form a "chaperone-like" assembly with a ferric siderophore complex with micromolar binding affinity (eq 3) led us to expand our working hypothesis to include the possibility of an exchange mechanism for Fe^{3+} between the protein bound holo-siderophore and the apo-protein. This is illustrated in eq 6, where "sid" indicates both native and xeno-siderophores, and Y represents either a siderophore or an opportunistic environmental synergistic anion. Such a process may represent a key step in the iron transport mechanism to the cytoplasm.

$$\text{holo-sid} + \text{apo-FbpA}_{Bp} \rightleftharpoons \text{apo-sid} + \text{Fe–FbpA}_{Bp}\text{–Y}$$

$$(6)$$
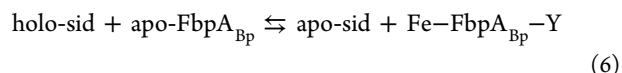
To test this extended hypothesis we performed time-dependent UV–vis spectroscopy experiments in which apo-FbpA$_{Bp}$ was added to ferric siderophore complexes, and the characteristic CT band for the ferric siderophore was monitored over time. Exchange of Fe^{3+} from the siderophore into the FbpA$_{Bp}$ binding site will change the position/intensity of the ferric siderophore CT band due to a donor group change in the first coordination shell of the Fe^{3+}.

For all ferric xeno-siderophore complexes investigated, the characteristic ligand-to-metal charge transfer band remained constant in position and intensity, even after exposure to apo-FbpA$_{Bp}$ for 3 h at pH 6.5 (Figure 4a). These results indicated that there is no change of the ferric siderophore first coordination shell in the presence of the protein and discounts an exchange reaction as described in eq 6. This observation is not surprising, given that the stability constants for the holo-siderophore complexes (~10^{23}–10^{49} M^{-1}),[3,4] are much higher than the Fe^{3+} association constant observed for holo-FbpA$_{Bp}$ (~10^{16} M^{-1}) (Table 1). However, a conformational change destabilizing the iron-siderophore binding pocket in the presence of a small-molecule chelator could facilitate dissociation of the Fe^{3+} into the protein binding pocket. In order to test this hypothesis for the iron-exchange reaction shown in eq 6, we carried out the reaction in the presence of biologically relevant anions. Our choice of anions was citrate and phosphate, which either form stable Fe–FbpA$_{Bp}$–X complexes or have been shown to facilitate the insertion of Fe^{3+} into *N. gonorrheae* FbpA, respectively.[59] Even in the presence of 50-fold excess of either of these anions there was no exchange of Fe^{3+} between a xeno-siderophore and FbpA$_{Bp}$. On the basis of these observations we conclude that FbpA$_{Bp}$ is unable to remove Fe^{3+} from a ferric xeno-siderophore or detectably alter the first coordination shell of Fe^{3+} under the *in vitro* conditions used.
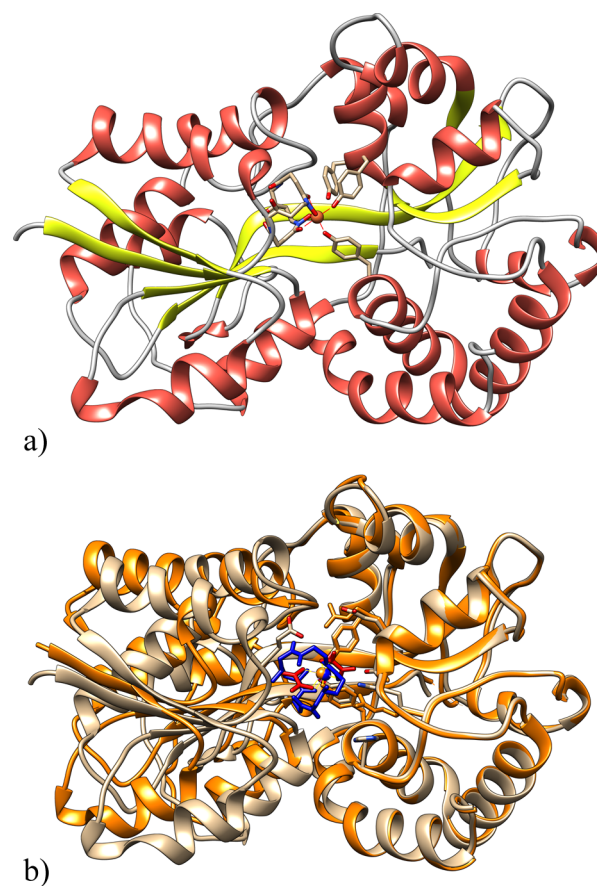
The results were quite different for the reaction between apo-FbpA$_{Bp}$ and holo-ALC, the native siderophore produced and utilized by the *Bordetellae*. At our experimental conditions the predominant species for holo-ALC is Fe$_2$(ALC)$_3$ (see SI), which is the expected *in vivo* form of the ferric siderophore and is hypothesized to be the form of the complex recognized by the outer membrane receptor FauA.[36,44,60] The ligand-to-metal CT band characteristic of Fe$_2$(ALC)$_3$ occurs at 428 nm, whereas the mononuclear species Fe(ALC)(OH$_2$)$_2^+$, which predominates at pH < 1, absorbs at longer wavelengths, λ_{max} = 500 nm.[44] Immediately after Fe$_2$(ALC)$_3$ was mixed with a solution of apo-FbpA$_{Bp}$ the λ_{max} shifted from 428 to 410 nm (Figure 4b). As reported in Table 1, Fe–FbpA$_{Bp}$–carbonate exhibits an absorption peak at 412 nm. The possibility of

a)

b)
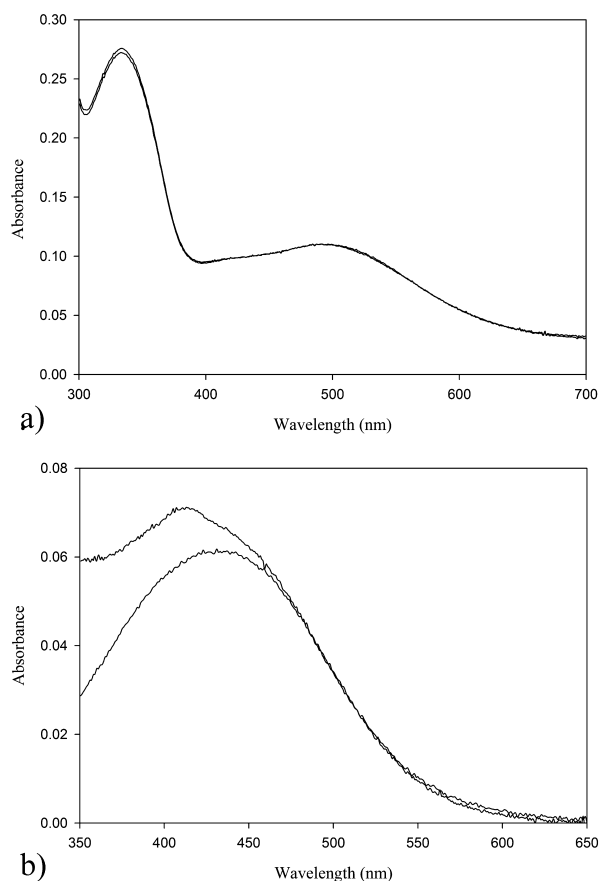
Figure 4. (a) UV−vis spectra with charge transfer (CT) band at 493 nm for Fe-ENT (15.4 μM) before and after addition of FbpA$_{Bp}$ (7.5 μM) in 50 mM MES, 100 mM NaCl at pH 6.5; (b) UV−vis spectra for Fe$_2$(ALC)$_3$ (9 μM) before and after addition of apoFbpA$_{Bp}$ (18 μM) showing a shift in λ_{max} from 428 nm (CT band for Fe$_2$ALC$_3$) to 410 nm. The mixture of Fe$_2$(ALC)$_3$ and FbpA$_{Bp}$ was monitored for 3 h, and the spectrum displayed here is from the end of that incubation.

a)

b)

Figure 5. Panel (a): Model of Fe-ALC in the binding cleft of FbpA$_{Bp}$ (2WOT); ERRAT score 95.425. Docked structure created with Patchdock using 2OWT as receptor and the ferric-alcaligin monomer (obtained from CCDC: C00080) as ligand. Panel (b): Model of Fe−FbpA$_{Bp}$−ALC superimposed on the crystal structure of Fe−FbpA$_{Bp}$−(oxalate)$_2$ (2OWS); 2OWS is shown in orange, the two oxalate anions are red, FbpA$_{Bp}$ is tan, and alcaligin is blue. Structures were aligned using the "Matchmaker" utility in Chimera. RMSD: 0.578 Å.

forming a carbonate complex was eliminated by the observation that this 410 nm peak appeared even in the absence of carbonate (degassed sample of Fe$_2$(ALC)$_3$ was mixed with degassed apo-FbpA$_{Bp}$ under an argon blanket). The appearance of this new absorption peak can be interpreted as due to a perturbation of the first coordination shell of Fe^{3+} in Fe$_2$(ALC)$_3$ as a result of binding with FbpA$_{Bp}$. This change of environment for Fe^{3+} could simply be due to a binding interaction between the protein and the holo-siderophore or could be indicative of the first step of iron release from Fe$_2$(ALC)$_3$, which requires reorganization of the Fe(III) first coordination shell. As noted above, the fluorescence emission quenching experiment involving apo-FbpA$_{Bp}$ and Fe$_2$(ALC)$_3$ also shows a lower K_d value, and a movement of the tryptophan residues from hydrophilic to hydrophobic environment ($\Delta\lambda_{emission} \approx 8$ nm; Figure 3a) compared to xeno-siderophore and apo-FbpA$_{Bp}$ interactions. These changes in the UV−vis and fluorescence spectral band positions and the greater observed affinity of FbpA$_{Bp}$ for the native siderophore (compared to the affinity with xeno-siderophores) suggest that reaction of Fe$_2$ALC$_3$ with apo-FbpA$_{Bp}$ may result in the formation of a precursor complex to Fe-FbpA$_{Bp}$-ALC under our experimental conditions.

Our modeling study shows the feasibility of the formation of Fe−FbpA$_{Bp}$−ALC as shown in Figure 5a. In our model ALC

serves as the "synergistic anion" in the exchange of Fe^{3+} from Fe$_2$ALC$_3$ to FbpA$_{Bp}$. This may represent a step in the process of delivering iron to the cytosol. In Figure 5b we have superimposed the model of Fe−FbpA$_{Bp}$−ALC on the reported crystal structure of Fe−FbpA$_{Bp}$−(oxalate)$_2$ (PDB: 2OWS). Both the model and the crystal structure show Fe^{3+} sequestered by two conserved tyrosine residues from FbpA$_{Bp}$ and the rest of the octahedral geometry first coordination shell occupied by an "external ligand" or synergistic anion (either ALC or two oxalate anions). The model fits very well with the crystal structure (RMSD 0.578 Å) and shows that in the model the ALC backbone can interact with the same amino acid residues that interact with the two oxalates in the crystal structure (Arg137 (2.67 Å); Asp179 (4.23 Å); Tyr200 (2.42 Å), Tyr143 (2.79 Å)). Two additional anion−protein interactions are predicted by the model of Fe−FbpA$_{Bp}$−ALC (Glu15 (1.42 Å) and His141 (4.25 Å)). This superposition between the modeled structure and the crystal structure of 2OWS strongly supports the feasibility of forming a Fe−FbpA$_{Bp}$−ALC assembly and may explain the appearance of the 410 nm band in our Fe^{3+}-exchange experiment.

■ CONCLUSION

The results presented here demonstrate a previously unde-scribed dual capacity for a periplasmic iron-uptake protein. $FbpA_{Bp}$ is capable of tightly binding unchelated Fe^{3+} directly in the presence of synergistic anions *in vitro* ($K'_{eff} \approx 10^{16}$ M^{-1}) and can also bind the native ferric siderophore $(Fe_2(ALC)_3)$ and ferric xeno-siderophore complexes with 0.1 and 1.0 μM affinities, respectively. Furthermore, $Fe_2(ALC)_3$ binding by $FbpA_{Bp}$ perturbs the coordination of Fe^{3+} in the native alcaligin siderophore complex in such a manner as to indicate partial dislocation of Fe^{3+} to the $FbpA_{Bp}$ binding site. This observation suggests a possible iron removal mechanism. These novel abilities are consistent with *Bordetella* studies showing that $FbpA_{Bp}$ is required by these respiratory pathogens for the utilization of both inorganic iron and siderophore-bound iron.[42] Our report describes the unique and opportunistic binding modes of *Bordetella* FbpA, hints at the possible function of this promiscuity, and begs the question, can other PBPs involved in iron-uptake bind iron both directly and indirectly?

■ ASSOCIATED CONTENT

Ⓢ Supporting Information

A summary of the iron(III) coordination chemistry of ALC, protein modeling and docking, fluorescence data, protein gel, and amino acid residue comparison. This material is available free of charge via the Internet at http://pubs.acs.org.

■ AUTHOR INFORMATION

Corresponding Author

*E-mail: Alvin.Crumbliss@duke.edu. Tel.:919-660-1540.

Notes

The authors declare no competing financial interest.

■ ACKNOWLEDGMENTS

■ ABBREVIATIONS

Fe^{3+}, Ferric iron; $FbpA_{Bp}$, ferric binding protein from *Bordetella pertussis*; $FbpA_{Ng}$ ferric binding protein from *Neisseria gonorrheae*; Fe-$FbpA_{Bp}$-X (X = carbonate, oxalate, NTA, or citrate), Fe^{3+} complex of $FbpA_{Bp}$ where both the protein and the anion (X) are in the first coordination shell of iron; Fe-siderophore or Fe-sid, ferric ion completely sequestered by the siderophore; $FbpA_{Bp}$(Fe-siderophore) or $FbpA_{Bp}$(Fe-sid), $FbpA_{Bp}$ chaperone complex of Fe-siderophore where the protein only interacts at the second coordination shell of iron; Fe-$FbpA_{Bp}$-siderophore or Fe-$FbpA_{Bp}$-sid, Fe^{3+} complex of $FbpA_{Bp}$ where both the protein and the siderophore occupy first coordination shell of iron; ALC, alcaligin; FC, ferrichrome; ENT, enterobactin; DFB, desferrioxamine B; Q%, percent fluorescence quenching; Q_{max}, maximum percent fluorescence quenching

■ REFERENCES

(1) Crichton, R. (2001) *Inorganic Biochemistry of Iron Metabolism: From Molecular Mechanisms to Clinical Consequences,*, 2nd ed., John Wiley & Sons, Ltd., Chichester.

(2) Chu, B. C., Garcia-Herrero, A., Johanson, T. H., Krewulak, K. D., Lau, C. K., Peacock, R. S., Slavinskaya, Z., and Vogel, H. J. (2010) Siderophore uptake in bacteria and the battle for iron with the host; a bird's eye view. *BioMetals 23*, 601−611.

(3) Raymond, K. N., and Dertz, E. A. (2004) Biochemical and physical properties of siderophores, in *Iron Transport in Bacteria* (Crosa, J. H., Mey, A. R, and Payne, S. M., Eds.), pp 3−17, ASM Press, Washington DC.

(4) Crumbliss, A. L., and Harrington, J. M. (2009) Iron sequestration by small molecules: thermodynamic and kinetic studies of natural siderophores and synthetic model compounds. *Adv. Inorg. Chem. 61*, 179−250.

(5) Harrington, J. M., and Crumbliss, A. L. (2009) The redox hypothesis in siderophore-mediated iron uptake. *BioMetals 22*, 679−689.

(6) Sandy, M., and Butler, A. (2009) Microbial iron acquisition: marine and terrestrial siderophores. *Chem. Rev. 109*, 4580−4595.

(7) Wandersman, C., and Stojiljkovic, I. (2000) Bacterial heme sources: the role of heme, hemoprotein receptors and hemophores. *Curr. Opin. Microbiol. 3*, 215−220.

(8) Genco, C. A., and White-Dixon, D. (2001) Emerging strategies in microbial haem capture. *Mol. Microbiol. 39*, 1−11.

(9) Schryvers, A. B., and Morris, L. J. (1988) Identification and characterization of the human lactoferrin-binding protein from *Neisseria meningitides*. *Infect. Immun. 56*, 1144−1149.

(10) Cornelissen, C. N., Biswas, G. D., Tsai, J., Paruchuri, D. K., Thompson, S. A., and Sparling, P. F. (1992) Gonococcal transferrin-binding protein 1 is required for transferrin utilization and is homologous to TonB-dependent outer membrane receptors. *J. Bacteriol. 174*, 5788−5797.

(11) Biswas, G. D., and Sparling, P. F. (1995) Characterization of *lbpA*, the structural gene for a lactoferrin receptor in *Neisseria gonorrhoeae*. *Infect. Immun. 63*, 2958−2967.

(12) Mietzner, T. A., Tencza, S. B., Adhikari, P., Vaughan, K. G., and Nowalk, A. J. (1998) Fe(III) periplasm-to-cytosol transporters of Gram-negative pathogens. *Curr. Top. Microbiol. Immunol. 225*, 114−135.

(13) Postle, K., and Larsen, R. A. (2007) TonB-dependent energy transduction between outer and cytoplasmic membranes. *BioMetals 20*, 453−465.

(14) Berntsson, R. P., Smits, S. H., Schmitt, L., Slotboom, D. J., and Poolman, B. (2010) A structural classification of substrate-binding proteins. *FEBS Lett. 584*, 2606−2617.

(15) Chu, B. C. H., and Vogel, H. J. (2011) A structural and functional analysis of Type III periplasmic and substrate binding proteins: their role in bacterial siderophore and heme transport. *Biol. Chem. 392*, 39−52.

(16) Miethke, M. (2013) Molecular strategies of microbial iron assimilation: from high-affinity complexes to cofactor assembly systems. *Metallomics 5*, 15−28.

(17) Fukami-Kobayashi, K., Tateno, Y., and Nishikawa, K. (1999) Domain dislocation: a change of core structure in periplasmic binding proteins in their evolutionary history. *J. Mol. Biol. 286*, 279−290.

(18) Tam, R., and Saier, M. H., Jr. (1993) Structural, functional, and evolutionary relationships among extracellular solute-binding receptors of bacteria. *Microbiol. Rev. 57*, 320−346.

(19) Parker Siburt, C. J., Mietzner, T. A., and Crumbliss, A. L. (2012) FbpA: a bacterial transferrin with more to offer. *Biochim. Biophys. Acta, Gen. Subj.- Special Issue on the Transferrins 1820*, 379−392.

(20) Chen, C. Y., Berish, S. A., Morse, S. A., and Mietzner, T. A. (1993) The ferric iron-binding protein of pathogenic *Neisseria* spp. functions as a periplasmic transport protein in iron acquisition from human transferrin. *Mol. Microbiol. 10*, 311−318.

(21) Parker Siburt, C. J., Roulhac, P. L., Weaver, K. D., Noto, J. M., Mietzner, T. A., Cornelissen, C. N., Fitzgerald, M. C., and Crumbliss,

A. L. (2009) Hijacking transferrin bound iron: protein-receptor interactions essential for iron transport. *N. gonorrhoeae. Metallomics 1*, 249−255.

(22) Banerjee, S., Parker Siburt, C. J., Mistry, S., Noto, J., DeArmond, P., Fitzgerald, M. C., Lambert, L. A., Cornelissen, C. N., and Crumbliss, A. L. (2012) Evidence of Fe^{3+} interaction with the plug domain of the outer membrane transferrin receptor protein of *Neisseria gonorrhoeae*: implications for Fe transport. *Metallomics 4*, 361−372.

(23) Dhungana, S., Taboy, C. H., Anderson, D. S., Vaughan, K. G., Aisen, P., Mietzner, T. A., and Crumbliss, A. L. (2003) The influence of the synergistic anion on iron chelation by ferric binding protein, a bacterial transferrin. *Proc. Natl. Acad. Sci. U.S.A. 100*, 3659−3664.

(24) Guo, M., Harvey, I., Yang, W., Coghill, L., Campopiano, D. J., Parkinson, J. A., MacGillivray, R. T., Harris, W. R., and Sadler, P. J. (2003) Synergistic anion and metal binding to the ferric ion-binding protein from *Neisseria gonorrhoeae*. *J. Biol. Chem. 278*, 2490−2502.

(25) Angerer, A., Gaisser, G., and Braun, V. (1990) Nucleotide sequences of the *sfuA*, *sfuB* and *sfuC* genes of *Serratia marcescens* suggest a periplasmic-binding-protein-dependent iron transport mechanism. *J. Bacteriol. 172*, 572−578.

(26) Tom-Yew, S. A. L., Cui, D. T., Bekker, E. G., and Murphy, M. E. (2005) Anion-independent iron coordination by the *Campylobacter jejuni* ferric binding protein. *J. Biol. Chem. 280*, 9283−9290.

(27) Tom-Yew, S. A. L. (2008) Ph. D. Dissertation, The University of British Columbia, Vancouver, BC.

(28) Shouldice, S. R., McRee, D. E., Dougan, D. R., Tari, L. W., and Schryvers, A. B. (2005) Novel anion-independent iron coordination by members of a third class of bacterial periplasmic ferric ion-binding proteins. *J. Biol. Chem. 280*, 5820−5827.

(29) Clarke, T. E., Ku, S. Y., Dougan, D. R., Vogel, H. J., and Tari, L. W. (2000) The structure of the ferric siderophore binding protein FhuD complexed with gallichrome. *Nat. Struct. Biol. 7*, 287−291.

(30) Carter, D. M., Miousse, I. R., Gagnon, J. N., Martinez, E., Clements, A., Lee, J., Hancock, M. A., Gagnon, H., Pawelek, P. D., and Coulton, J. W. (2006) Interactions between TonB from *Escherichia coli* and the periplasmic protein FhuD. *J. Biol. Chem. 281*, 35413−24.

(31) Rohrbach, M. R., Braun, V., and Köster, W. (1995) Ferrichrome transport in *Escherichia coli* K-12: Altered substrate specificity of mutated periplasmic FhuD and interaction of FhuD with the integral membrane protein FhuB. *J. Bacteriol. 177*, 7186−7193.

(32) Bordet, J., and Gengou, O. (1906) Le microbe de la coqueluche. *Ann. Inst. Pasteur (Paris) 20*, 731−741.

(33) Mattoo, S., and Cherry, J. D. (2005) Molecular pathogenesis, epidemiology, and clinical manifestations of respiratory infections due to *Bordetella pertussis* and other *Bordetella* subspecies. *Clin. Microbiol. Rev. 18*, 326−382.

(34) Vanderpool, C. K., and Armstrong, S. K. (2001) The *Bordetella bhu* locus is required for heme iron utilization. *J. Bacteriol. 183*, 4278−4287.

(35) Moore, C. H., Foster, L. A., Gerbig, D. G., Jr., Dyer, D. W., and Gibson, B. W. (1995) Identification of alcaligin as the siderophore produced by *Bordetella pertussis* and *B. bronchiseptica*. *J. Bacteriol. 177*, 1116−1118.

(36) Brickman, T. J., Hansel, J. G., Miller, M. J., and Armstrong, S. K. (1996) Purification, spectroscopic analysis and biological activity of the macrocyclic dihydroxamate siderophore alcaligin produced by *Bordetella pertussis* and *Bordetella bronchiseptica*. *BioMetals 9*, 191−203.

(37) Beall, B., and Hoenes, T. (1997) An iron-regulated outer-membrane protein specific to *Bordetella bronchiseptica* and homologous to ferric siderophore receptors. *Microbiology 143*, 135−145.

(38) Beall, B., and Sanden, G. N. (1995) A *Bordetella pertussis fepA* homologue required for utilization of exogenous ferric enterobactin. *Microbiology 141*, 3193−3205.

(39) Brickman, T. J., Anderson, M. T., and Armstrong, S. K. (2007) *Bordetella* iron transport and virulence. *BioMetals 20*, 303−322.

(40) Brickman, T. J., and Armstrong, S. K. (2009) Temporal signaling and differential expression of *Bordetella* iron transport

systems: The role of ferrimones and positive regulators. *BioMetals 22*, 33−41.

(41) Anderson, M. T., and Armstrong, S. K. (2004) The BfeR regulator mediates enterobactin-inducible expression of *Bordetella* enterobactin utilization genes. *J. Bacteriol. 186*, 7302−7311.

(42) Brickman, T. J., Cummings, C. A., Liew, S.-Y., Relman, D. A., and Armstrong, S. K. (2011) Transcriptional profiling of the iron starvation response in *Bordetella pertussis* provides new insights into siderophore utilization and virulence gene expression. *J. Bacteriol. 193*, 4798−4812.

(43) Hou, Z., Sunderland, C. J., Nishio, T., and Raymond, K. N. (1996) The first structure of a ferric dihydroxamate siderophore. *J. Am. Chem. Soc. 118*, 5148−5149.

(44) Hou, Z., Raymond, K. N., O'Sullivan, B., Esker, T. W., and Nishio, T. (1998) A preorganized siderophore: Thermodynamic and structural characterization of alcaligin and bisucaberin, microbial macrocyclic dihydroxamate-chelating agents. *Inorg. Chem. 37*, 6630−6637.

(45) Stock, J. B., Rauch, B., and Rosaman, S. (1977) Periplasmic space in *Salmonella typhimurium* and *Escherichia coli*. *J. Biol. Chem. 252*, 7850−7861.

(46) Wilks, J. C., and Slonczewski, J. L. (2007) pH of the cytoplasm and periplasm of *Escherichia coli*: Rapid measurement by green fluorescent protein fluorimetry. *J. Bacteriol. 189*, 5601−5607.

(47) Neilands, J. B., and Nakamura, K. (1991) Detection, determination, isolation, characterization, and regulation of microbial iron chelates, in *CRC Handbook of Microbial Iron Chelates* (Winkelmann, G., Ed.), pp 1−14, CRC Press, London, England.

(48) Stainer, D., and Scholte, M. (1971) A simple chemically defined medium for the production of phase I *Bordetella pertussis*. *J. Gen. Microbiol. 63*, 211−220.

(49) Shouldice, S. R., Dougan, D. R., Skene, R. J., Tari, L. W., McRee, D. E., Yu, R.-h., and Schryver, A. B. (2003) High resolution structure of an alternate form of the ferric iron binding protein from *Haemophilus influenza*. *J. Biol. Chem. 278*, 11513−11519.

(50) Bradford, M. M. (1976) A rapid and sensitive method for the quantitation of microgram quantities of protein utilizing the principles of protein-dye binding. *Anal. Biochem. 72*, 248−254.

(51) Reshetnyak, Y. K., and Burstein, E. A. (2001) Decomposition of protein tryptophan fluorescence spectra into log-normal components. II. The statistical proof of discreteness of tryptophan classes in proteins. *Biophys. J. 81*, 1710−1734.

(52) Matveeva, E. G., Morisseau, C., Goodrow, M. H., Mullin, C., and Hammock, B. D. (2009) Tryptophan fluorescence quenching by enzyme inhibitors as a tool for enzyme active site structure investigation: epoxide hydrolase. *Curr. Pharm. Biotechnol. 10*, 589−599.

(53) Sprencel, C., Cao, Z., Qi, Z., Scott, D. C., Montague, M. A., Ivanoff, N., Xu, J., Raymond, K. N., Newton, S. M. C., and Klebba, P. E. (2000) Binding of ferric enterobactin by the *Escherichia coli* periplasmic protein FepB. *J. Bacteriol. 182*, 5359−5364.

(54) Dhungana, S., White, P. S., and Crumbliss, A. L. (2001) Crystal structure of ferrioxamine B: A comparative analysis and implications for molecular recognition. *J. Biol. Inorg. Chem. 6*, 810−818.

(55) Schneidman-Duhovny, D., Inbar, Y., Nussinov, R., and Wolfson, H. J. (2005) PatchDock and SymmDock: Servers for rigid and symmetric docking. *Nucleic Acids Res. 33*, W363−367.

(56) Pettersen, E. F., Goddard, T. D., Huang, C. C., Couch, G. S., Greenblatt, D. M., Meng, E. C., and Ferrin, T. E. (2004) UCSF Chimera – A visualization system for exploratory research and analysis. *J. Comput. Chem. 25*, 1605−1612.

(57) Colovos, C., and Yeates, T. O. (1993) Verification of protein structures: Patterns of nonbonded atomic interactions. *Protein Sci. 2*, 1511−1519.

(58) Bruns, C. M., Nowalk, A. J., Arvai, A. S., McTigue, M. A., Vaughan, K. G., Mietzner, T. A., and McRee, D. E. (1997) Structure of *Haemophilus influenzae*: Fe^{3+}-binding protein reveals convergent evolution within a superfamily. *Nat. Struct. Biol. 4*, 919−924.

(59) Weaver, K. D., Gabricević, M., Anderson, D. S., Adhikari, P., Mietzner, T. A., and Crumbliss, A. L. (2010) Role of citrate and

phosphate anions in the mechanism of iron(III) sequestration by ferric binding protein: Kinetic studies of the formation of the holoprotein of wild-type FbpA and its engineered mutants. *Biochemistry 49*, 6021–6032.

(60) Brickman, T. J., and Armstrong, S. K. (1999) Essential role of the iron-regulated outer membrane receptor FauA in alcaligin siderophore-mediated iron uptake in *Bordetella* species. *J. Bacteriol. 181*, 5958–5966.